Supplementary Figures

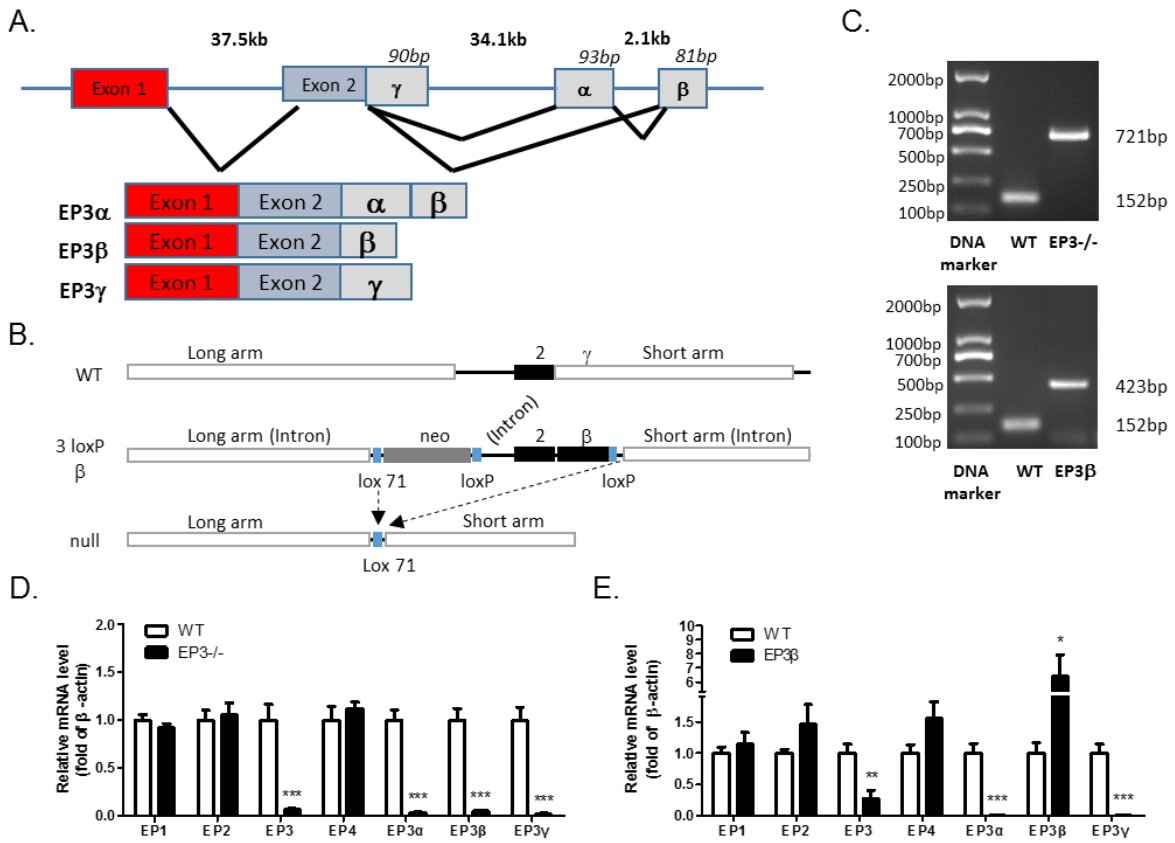

Supplementary Figure S1. **Gene structure of mouse EP3 gene and generation and validation of the EP3 gene deficient mice. A)** Gene structure of the EP3 gene and three isoforms via alternative splicing. Exon 1 and exon 2 are common in all three EP3 isoforms and cover most of the seven transmembrane regions. The splice variants of α, β and γ exons connect to the C-terminus of exon 2. The γ exon is contiguous with exon 2 in the genome. **B)** Comparison of the WT sequence altered by the correctly targeted 3 loxP EP3β knock-in vector, and the EP3 null allele after Cre deletion at the outermost loxP site. **C)** Genotyping of EP3-/- (721bp) and EP3β (423bp) alleles, and a common wild-type (152bp) allele by PCR. **D)** mRNA levels of the EP receptors in WT (n=5) and EP3-/- (n=6) mice. **E)** Expression of the EP3 receptors via real-time PCR in WT (n=6) and EP3β (n=6) mice. ***p*<0.01, ****p*<0.001 *vs.* WT mice.

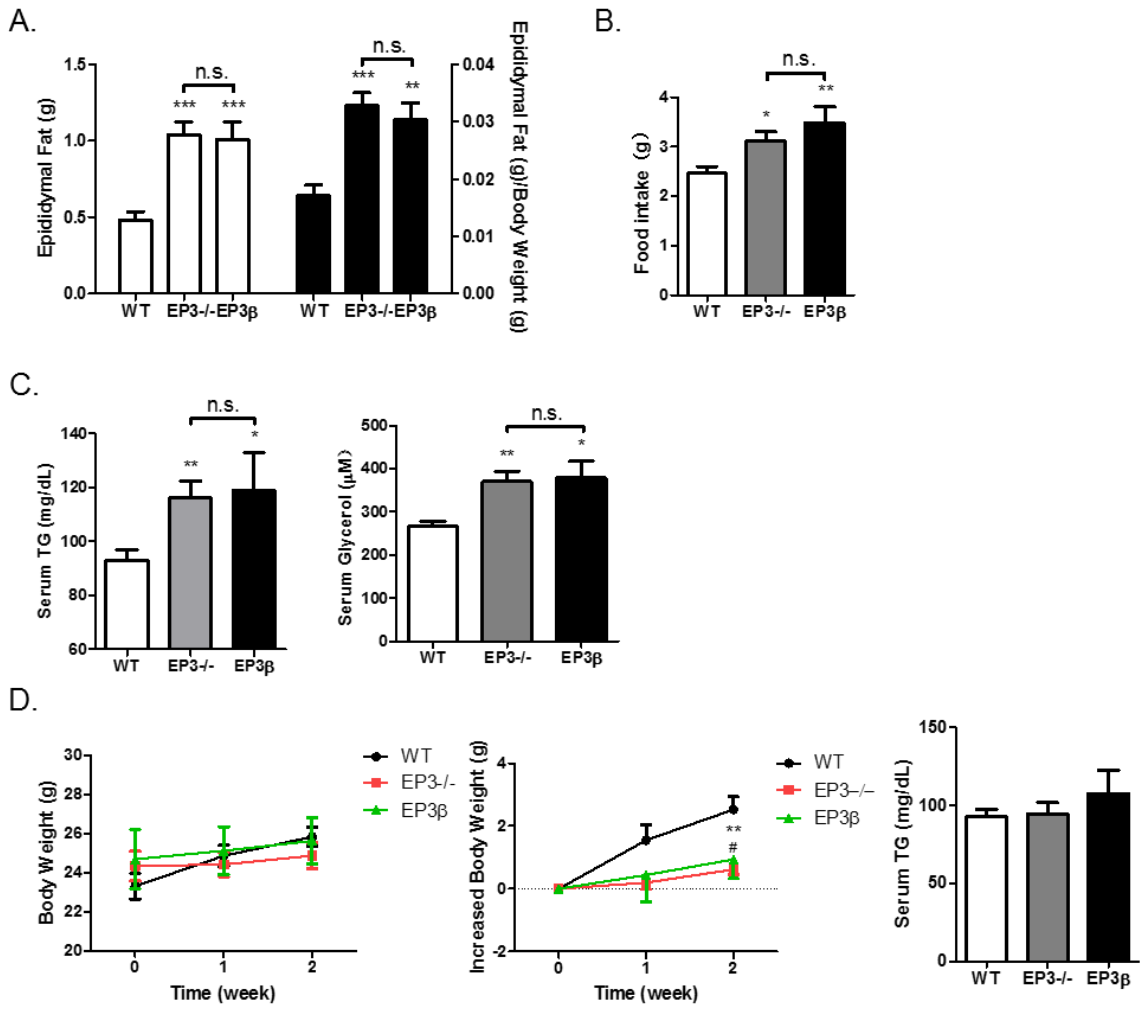

Supplementary Figure S2. The weight of epididymal fat pad, food intake and the food restriction test. A) Increased weight of epididymal WAT in the EP3-/- and EP3β mice. Epididymal white adipose tissue of WT (n=9), EP3-/- (n=6) and EP3β (n=8) mice was weighted and the ratio of epididymal fat mass to body weight was calculated. **B)** Food consumption of the EP3-/- and EP3β mice were increased. 24h food intake of WT (n=21), EP3-/- (n=8) and EP3β (n=7) mice were measured by metabolism cages. **C**) Increased TG and glycerol concentration in the serum of both EP3-/- and EP3β mice before they got obesity. The Serum TG and glycerol levels of WT (n=8), EP3-/- (n=7) and EP3β (n=4) mice were measured at the age of 8 weeks. **D)** The body weights and TG levels of EP3-/- and EP3β mice were controlled by the food intake. Both EP3-/- (n=6) and EP3β (n=5) mice showed stagnant body weights when the food intake was equal to the WT mice (n=11), and after two weeks of food restriction the TG concentration was down-regulated, and showed no significant difference to WT mice. The food restriction test was performed from the age of 8 weeks to 10 weeks. *p<0.05, **p<0.01, ***p<0.001 *vs.* WT mice. $^{\#}p$<0.05, EP3β *vs.* WT mice.

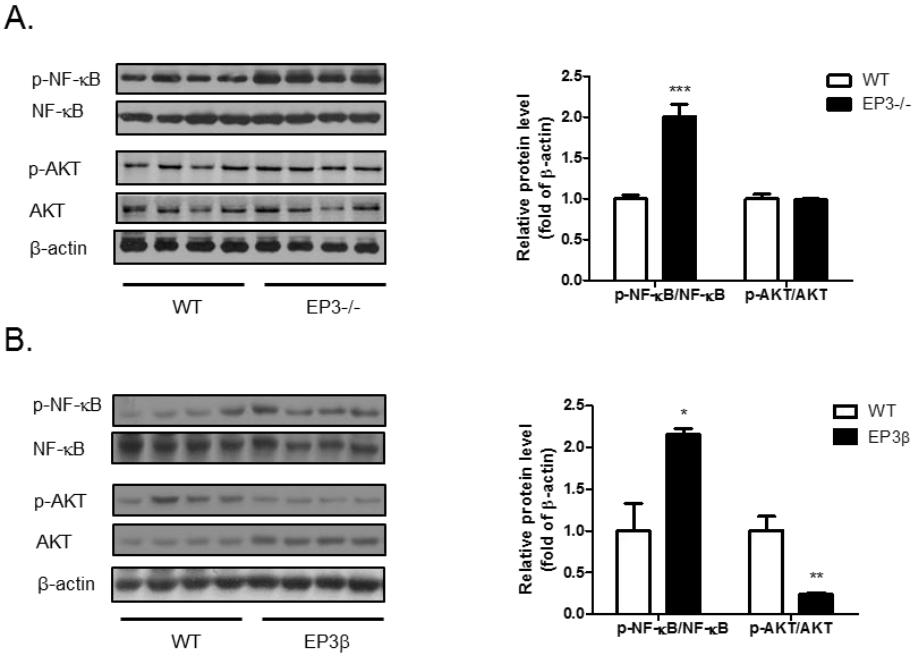

Supplementary Figure S3. The inflammation and insulin pathway were changed in EP3-/- mice and EP3β mice WAT. **A&B)** Increased inflammation and impaired insulin sensitivity in WAT of EP3-/- and EP3β mice at the age of 20 weeks. The protein levels of phospho-NF-κB, total NF-κB, phospho-AKT and total AKT in WT and the EP3-/- (**A**) or EP3β (**B**) mice epididymal fat were quantified by western blot. The right bargraph in (**A&B**) is the quantification of western blot. **p*<0.05, ***p*<0.01, ****p*<0.001 *vs.* WT mice.

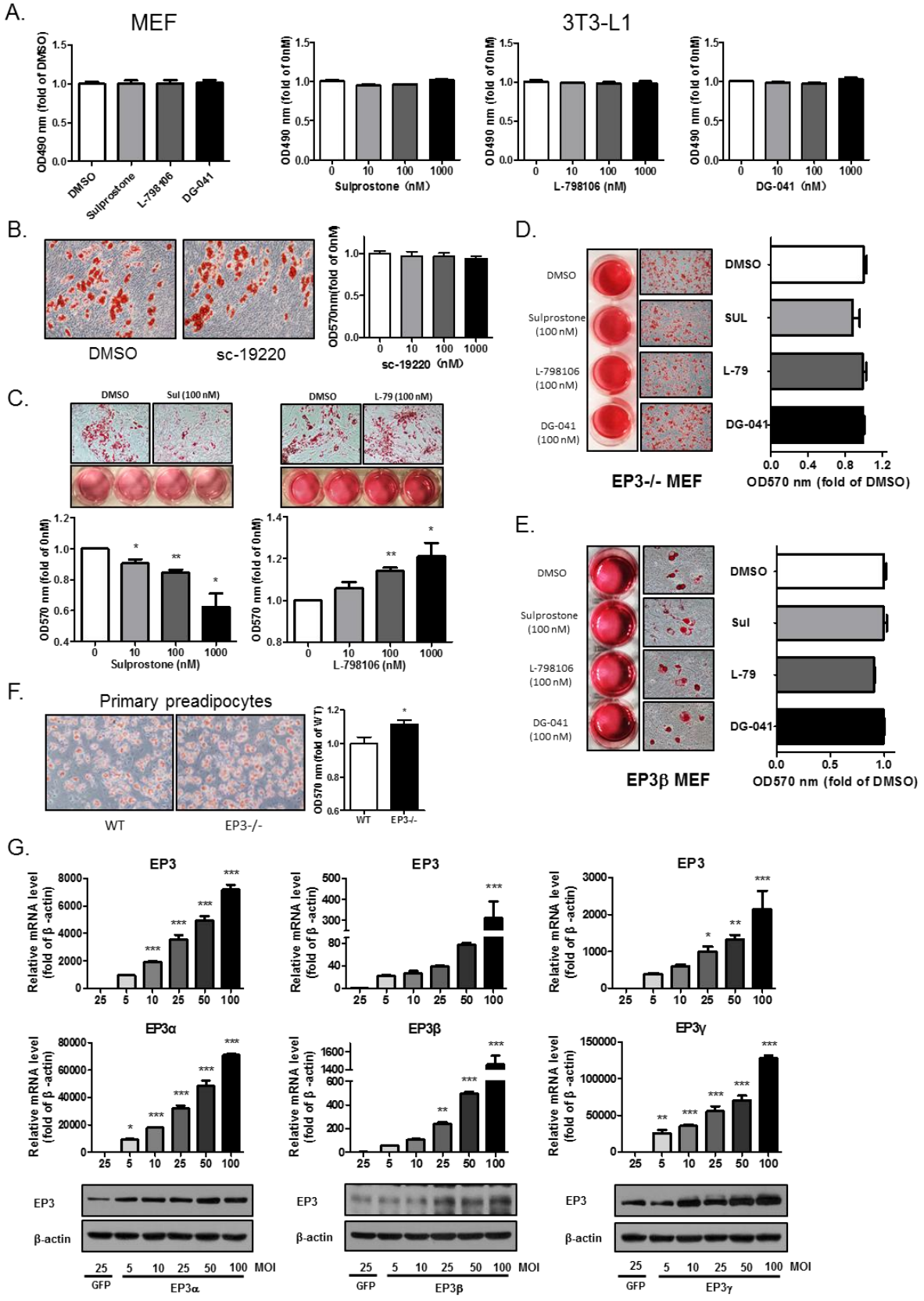

Supplementary Figure S4. Effect of the EP3 receptors in the differentiation of 3T3L1 cells and MEFs and generation of adenoviruses expressing GFP-tagged EP3α, EP3β

and EP3γ. A) Effect of activation or antagonism of EP3 on cell viability of MEFs and 3T3-L1 cells. MTT assay of MEFs or 3T3-L1 cells treated with DMSO, sulprostone, L-798106 or DG-041 for 24 hours. **B)** Effect of the EP1 antagonist sc-19220 on MEFs differentiation. No effect of sc-19220 treatment on MEFs' differentiation was evident. WT MEFs were pretreated with different concentrations of sc-19220 for 1 hour before the DMI induction. **C)** Effect of sulprostone or L-798106 on 3T3-L1 cells differentiation. 3T3-L1 cells were pretreated with different concentrations of sulprostone or L-79810 for 1 hour before the DMI induction. **D&E)** Effect of the EP3 agonist and antagonists on adipogenesis in MEFs of the EP3-/- mice and EP3β mice. The EP3 agonist or antagonists had little effect on the EP3-/- or EP3β MEFs' differentiation. MEFs of EP3-/- (**D**) or EP3β (**E**) embryos were cultured and pretreated with DMSO or 100nM sulprostone, L-798106 or DG-041 for 1 hour before the DMI induction. **F)** Increased adipogenesis of EP3-/- primary preadipocytes. Primary preadipocytes of WT and EP3-/- mice were cultured and differentiated. **G)** Verification of EP3α, EP3β and EP3γ adenoviruses. mRNA and protein identifications of ad-EP3α (left panels), ad-EP3β (middle panels) and ad-EP3γ (right panels) in HepG2 cell line. The mRNA levels of each isoform and protein levels of the EP3 receptors were tested for each adenovirus. For all the adipogenesis experiments, after 8 days of differentiation, Oil Red O staining was performed (**B-D**&**F** 200×, E 400×), followed by taking images or isopropanol dissolution. The absorption of dissolved Oil Red O was read under 570nm wavelength. *p<0.05, **p<0.01, ***p<0.001 *vs.* DMSO (**C**) or WT (**F**) or GFP (**G**), n=3 in each group.

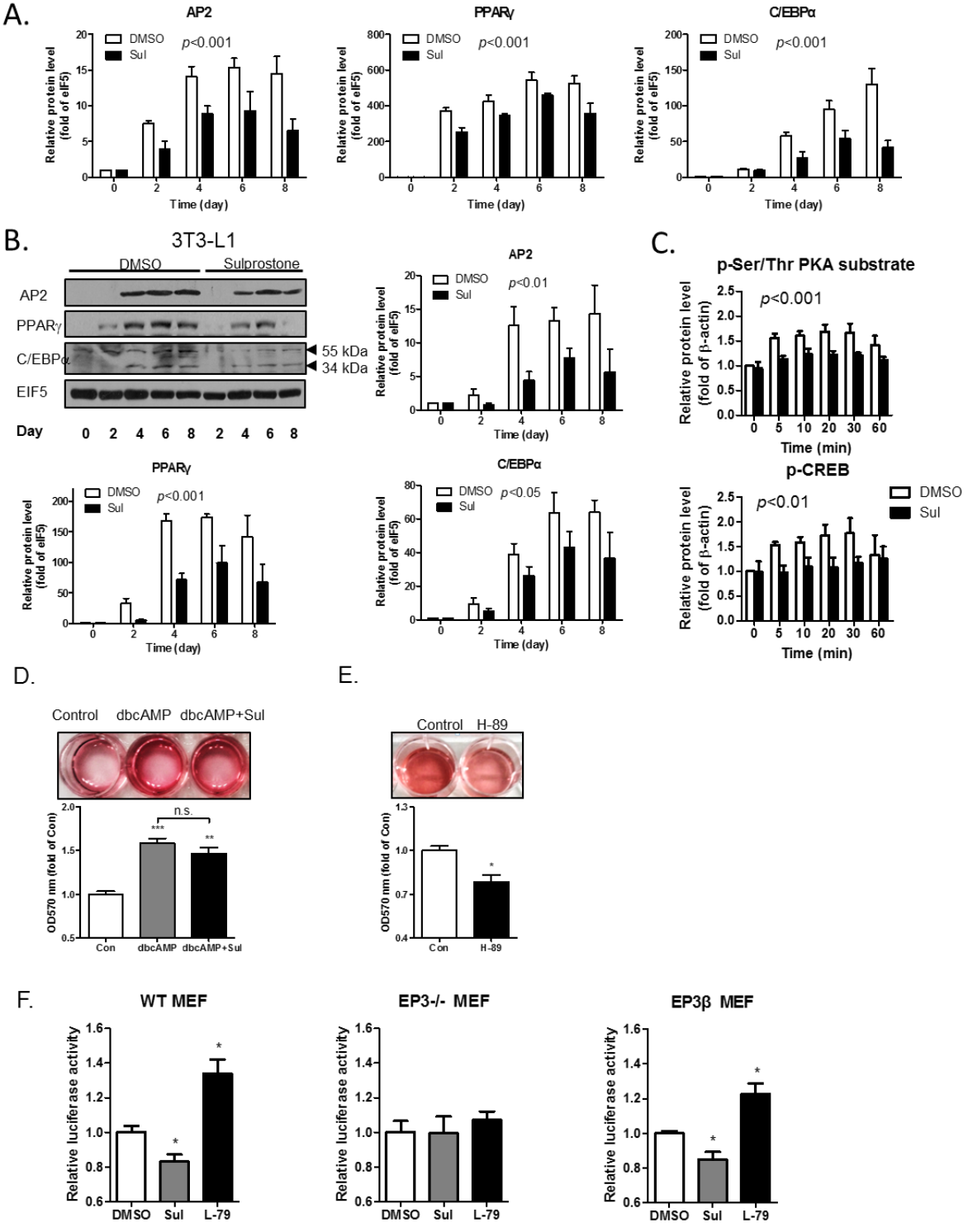

Supplementary Figure S5. Effects of EP3 in adipogenesis process and the EP3 ligands on intracellular cAMP levels. A) Statistical analysis of protein levels in Figure 4B. **B)** Effect of sulprostone treatment on adipogenic protein expression. Pretreatment of 3T3-L1 cells with 100nM sulprostone decreased protein levels of AP2, PPARγ and C/EBPα on different days. **C)** Statistical analysis of protein levels in Figure 4E. **D)** dbcAMP reversed the effect of sulprostone on primary preadipocyte differentiation. WT mouse primary

preadipocytes were pretreated with dbcAMP (0.5mM) or dbcAMP (0.5mM) plus sulprostone (1μM) before differentiation. No difference was found between dbcAMP group and dbcAMP plus sulprostone group. **E)** H-89 inhibited EP3-/- mouse primary preadipocytes differentiation. Primary preadipocytes of the EP3-/- mice were pretreated with DMSO or 1μM H-89 before differentiation. **F)** Effect of sulprostone and L-798106 on WT, EP3-/- and EP3β MEFs' cAMP contents. Relative luciferase activity of WT, EP3-/- and EP3β MEFs with sulprostone (100nM) or L-798106 (100nM) treatment were measured. *$p<0.05$, **$p<0.01$, ***$p<0.001$ *vs.* control, n=3-4 in each group.

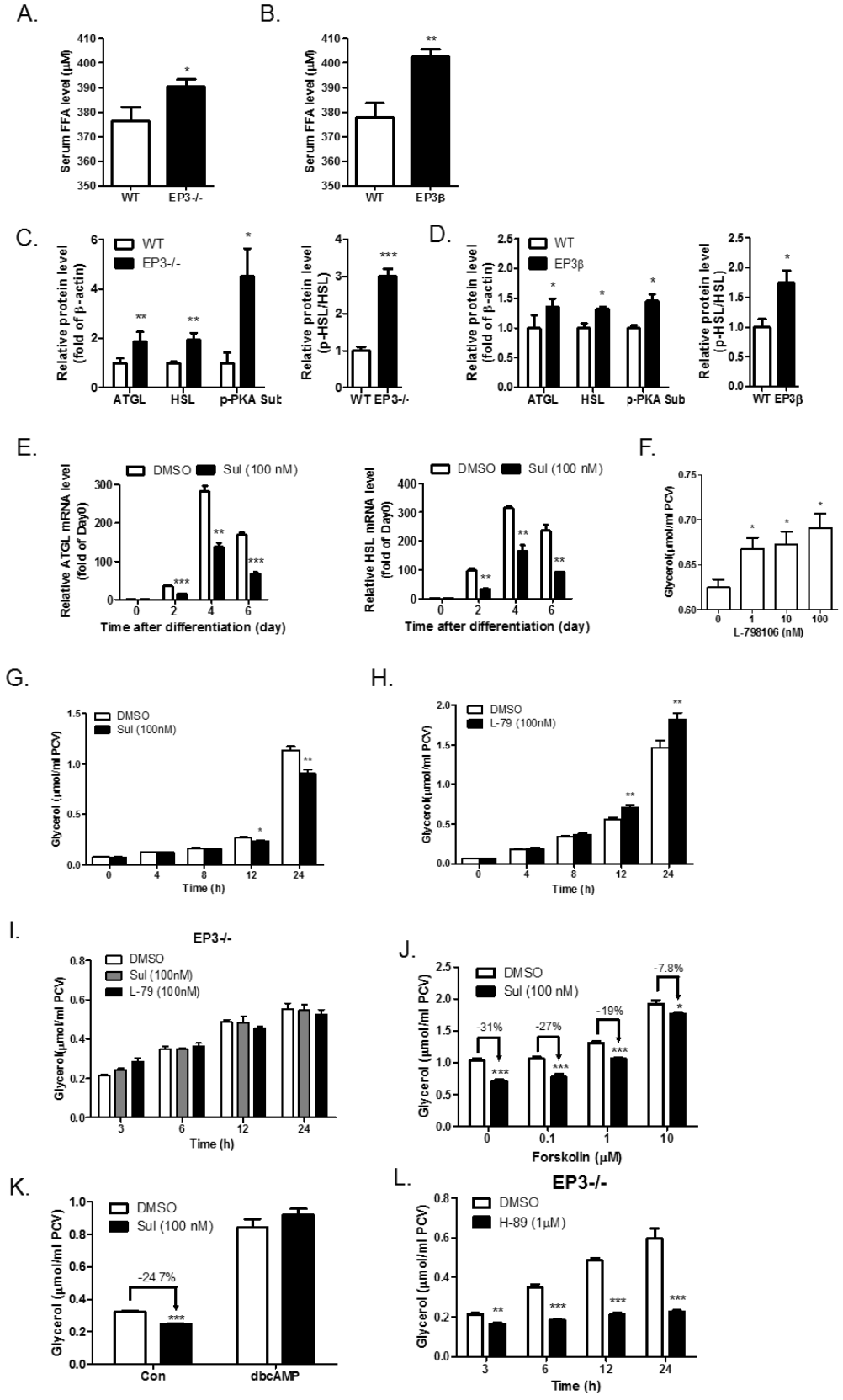

Supplementary Figure S6. Lipolysis in mice deficient for the EP3 receptors and in MEFs and adipocytes with altered EP3 activity. A&B) Increased serum free fatty acid

levels in the EP3-/- and EP3β mice at the age of 20 weeks. Serum free fatty acid (FFA) levels of WT (n=8) and the EP3-/- (n=9) mice were measured (**A**). FFA levels in WT (n=7) and the EP3β (n=6) mice (**B**). **C&D)** Statistical analysis of protein levels in Figure 5F (**C**) and Figure 5G (**D**). **E)** Effect of sulprostone treatment on mRNA expression of lipases in MEFs. Pretreated with 100nM sulprostone, the mRNA expression of ATGL and HSL from WT MEFs on day 0, 2, 4 and 6 was quantified by real-time PCR. Each gene was calculated by fold of day 0. **F)** Inhibition of EP3 by L-798106 increased lipolysis in rat adipocytes. Different concentrations of L-798106 treated rat primary mature adipocytes for 6 hours and the released glycerol was measured. **G&H)** The time-dependent effect of sulprostone or L-798106 treatment on lipolysis in rat adipocytes. Sulprostone (100nM) treated rat primary mature adipocytes and the released glycerol was measured at different time points (**G**). L-798106 (100nM) treated rat primary mature adipocytes and the released glycerol was measured at different time points (**H**). **I)** Sulprostone or L-798106 treatment had no effect on lipolysis of EP3-/- mouse adipocytes. 100nM sulprostone or L-798106 treated EP3-/- mouse primary mature adipocytes. The released glycerol was measured at different time points. **J&K)** Directly or indirectly increased cAMP content attenuated the sulprostone's suppressive effect on lipolysis. The glycerol concentration of rat primary mature adipocytes was measured after co-treatment with 100nM sulprostone and forskolin (**J**) or 0.5mM dbcAMP (**K**) for 12h. **L)** H-89 inhibited lipolysis in EP3-/- mouse primary mature adipocytes. Glycerol concentration in the culture medium of the EP3-/- mouse primary adipocytes treated with 1μM H-89 at different time points. *p<0.05, **p<0.01, ***p<0.001 *vs.* WT mice (**A-D**) or DMSO (**E-L**), n=3 in each group unless otherwise clarified.

Supplementary Tables

Supplementary Table S1: Genotyping PCR primers

Genes	Forward (5'→3')	Reverse (5'→3')
WT	GCTGTCTCCAGTTGCTCTA	TGCCTCAGTCCATAAGGGTTAGGG
EP3-/-	TGGCACAGAAAGGATTATCTA	AACGCTTGTCAAATGTTCAT
EP3β	ATAATGATGTTGAAAA-TGATC	TGTGTCGTCTTGCCCCCG

Supplementary Table S2: Real-time PCR primers

Genes	Forward (5'→3')	Reverse (5'→3')
EP1	TAACGATGGTCACGCGATGG	ATGCAGTAGTGGGCTTAGGG
EP2	ATGCTCCTGCTGCTTATCGT	AGGGCCTCTTAGGCTACTGC
EP4	GTTCCGAGACAGCAAAAGC	CACCCCGAAGATGAACATCAC
EP3	GGATCATGTGTGTGCTGTCC	GCAGAACTTCCGAAGAAGGA
EP3α	TAATTGCAGTTCGCCTGGCT	GGAGCTGGAAGCATAGTTGGT
EP3β	TAATTGCAGTTCGCCTGGCT	TCAGGTTGTTCATCATCTGGCA
EP3γ	GTGTGTGCTGTCCGTCTGTT	GGAGACAGCGTTTGCTACCTG
C/EBPα	GCAAAGCCAAGAAGTCGGTG	TCACTGGTCAACTCCAGCAC
C/EBPβ	GCTGAGCGACGAGTACAAGA	TTGAACAAGTTCCGCAGGGT
C/EBPδ	GCCATGTACGACGACGAGAG	GGTTGCTGTTGAAGAGGTCG
PPARγ	TTCGATCCGTAGAAGCCGTG	TCCTTGGCCCTCTGAGATGA
AP2	GCGTGGAATTCGATGAAATCA	CCCGCCATCTAGGGTTATGA
ATGL	AACACCAGCATCCAGTTCAA	GGTTCAGTAGGCCATTCCTC
HSL	ACCGAGACAGGCCTCAGTGTG	GAATCGGCCACCGGTAAAGAG
β-actin	AGCCATGTACGTAGCCATCC	GCTGTGGTGGTGAAGCTGTA

Supplementary Materials and methods

Generation of the EP3-/- and EP3β mice

To generate the EP3-/- and EP3β mice, wild-type allele was altered by the targeted 3 loxP EP3β knock-in vector, and the EP3 null allele was deleted by Cre at the outermost loxP sites. In detail, a 1,548 bp short homology arm was amplified encompassing exon 2, and the contiguous gamma C-terminal coding region was isolated. This fragment was subcloned into the ploxmPneo vector 3' to the most distal loxP site. A 6,790 bp long homology arm was amplified which was subloned into pCRII. This PCR product was excised with EcoRI at flanking EcoRI sites and the ends filled in with the Klenow fragment of DNA polymerase I. The resulting fragment was cloned into ploxmPneo in the SacI site which had also been filled. This placed the long homology arm 5' to the lox 71 site. The resulting 15 kb plasmid was linearized with NotI and transfected into TL1 129SvEv ES cells. Correctly targeted cells were identified and chimeras were generated with C57BL/6 blastocysts. Chimeric mice were backcrossed 10 generations onto the C57BL/6 background to generate EP3β mice. These mice were crossed with EIIa Cre mice that had been backcrossed more than 10 generations onto the C57BL/6 background to generate a global deletion and the resulting heterozygote progeny were backcrossed to C57BL/6 to select for the loss of the EIIa Cre allele and those progeny were intercrossed to generate homozygous null mice (Figure S1B). The detailed method for genotyping EP3-/- mice was described before (Chen et al., 2012). Briefly, they were identified by PCR with the tail genomic DNA, as well as the genotyping of wild-type (WT) and EP3β mice. The primers are listed in Supplementary table 1. PCR reactions were carried out at 94℃ for 30 seconds, 58℃ (EP3-/-) or 53℃ (EP3β) for 30 seconds, 72℃ for

30 seconds for 35 cycles for WT and EP3-/- or EP3β alleles. PCR products were separated with 1% agarose gel as showed in Figure S1C. This genotyping result was also confirmed by real-time PCR in other tissue including the WAT of WT, EP3-/-, and EP3β mice (Figure S1D&E).

Measurement of adipocyte size

Epididymal fat tissue sections were stained with Hematoxylin and Eosin (H&E). The diameters of adipocytes were measured using ImageJ software (NIH), and used to calculate the cell sizes with the formula $\pi*(\text{diameter}/2)^2$. The frequency of different sizes was figured up within a $100\mu m^2$-interval.

Protein immunoblotting

Proteins from adipose tissues or cells were extracted in lysis buffer, as previously described (Xu et al., 2009). Lysates containing 20-60μg of protein were subjected to SDS–PAGE and then transferred to PVDF membrane. Non-specific binding of antibody was blocked by washing with TBS buffer containing 10% milk for 1 h. The blots were then incubated with the primary antibody of phospho-HSL (1:1000 dilution), HSL (1:1000 dilution), ATGL (1:2000 dilution), phospho-(Ser/Thr) PKA substrate (1:1000 dilution), phospho-CREB (1:1000 dilution), CREB (1:1000 dilution), EP3 receptor (1:1000 dilution), AP2 (1:1000 dilution), PPARγ (1:1000 dilution) and C/EBPα (1:1000 dilution) overnight and then the HRP-conjugated secondary antibody for 1h. The blots were visualized using the chemiluminescent detection method (Pierce). The levels of proteins present on the blots were

quantified by densitometry using ImageJ (NIH).

mRNA Isolation, RT-PCR and Real-Time PCR.

Total mRNA was isolated with a commercial mRNA isolation kit (BioTeke). mRNA samples were reverse-transcribed to cDNA with RevertAid First Strand cDNA Synthesis Kit (Fermentas). cDNA was used as template in the real-time PCR reaction with SYBR Green 1 (Bio-Rad). The primers used in our study are listed in Supplementary Table 2. The real-time PCR reaction was carried out at 94 ℃ for 5 min, followed by 35 cycles of 94 ℃ for 30 s, 59 ℃ for 30 s, 72 ℃ for 30 s, with a final extension at 72 °C for 5 min. β-actin was used as an internal control.

MTT assay

MEF/3T3-L1 cells were seeded in 24-well plates at the concentration of 2×10^5 cells/well. After incubated in a 37℃ incubator overnight, the cells were then treated with the EP3 receptor agonist or antagonist for 20 hours. MTT solution (5 mg/ml) was added at a volume of 50μl in each well and was incubated for 4 hours. Finally, 150μl DMSO was used to mix with the cells for 10 min and the solution was removed into a 96-well plate. Absorbance values were measured at the wavelength of 570 nm.

Measurement serum TG and insulin levels

. Serum samples were obtained from mice for TG, TC and insulin measurement by using TG assay kit (BioSino) as we previously described (Li et al., 2011) or Insulin ELISA kit

(Millipore).

Glycerol and free fatty acid measurement

Serum samples and phenol red-free and serum-free DMEM samples collected from cultured adipose tissue or adipocytes were used to quantify glycerol with glycerol assay kit (Applygen). The concentration of glycerol was further evaluated to indicate the lipolysis states adjusted with PCV or tissue weight. Serum samples were used to quantify free fatty acid with FFA assay kit (Comin Bio). In brief, under weakly acidic conditions, the reaction of FFA and copper salt produced copper soap, which had a characteristic absorption peak at 715nm, and the content of free fatty acid in a certain range was linear with the degree of absorption.

Determination of VLDL-TG production *in vivo*

We quantified the rate of very-low-density lipoprotein (VLDL) secretion *in vivo* as described previously (Chang et al., 1999). Briefly, mice were injected tyloxapol (sigma, 500mg/kg in normal saline), a lipoprotein lipase inhibitor, after 6 hours fasting and monitored the serum TG prior to and after the injection at 1, 2, 3, and 4 hours.

Triglyceride clearance assay

Mice were injected with 0.25 ml of intralipid (Sigma) through the tail vein of mice and measured the serum TG concentration immediately after injection and followed by the time points of 30, 60, 120, 180 and 240 minutes.

References

Chang, B. H., Liao, W., Li, L., Nakamuta, M., Mack, D., and Chan, L. (1999). Liver-specific inactivation of the abetalipoproteinemia gene completely abrogates very low density lipoprotein/low density lipoprotein production in a viable conditional knockout mouse. J Biol Chem*, 274*, 6051-6055.

Chen, L., Miao, Y., Zhang, Y., et al. (2012). Inactivation of the E-prostanoid 3 receptor attenuates the angiotensin II pressor response via decreasing arterial contractility. Arterioscler Thromb Vasc Biol*, 32*, 3024-3032.

Li, J., Chi, Y., Wang, C., et al. (2011). Pancreatic-derived factor promotes lipogenesis in the mouse liver: role of the Forkhead box 1 signaling pathway. Hepatology*, 53*, 1906-1916.

Xu, C., He, J., Jiang, H., et al. (2009). Direct effect of glucocorticoids on lipolysis in adipocytes. Mol Endocrinol*, 23*, 1161-1170.